Towards the lattice effects on the holographic superconductor

Norihiro Iizuka[a] **and Kengo Maeda**[b]

[a] *Theory Division, CERN,*
CH-1211 Geneva 23, Switzerland

[b] *Faculty of Engineering, Shibaura Institute of Technology,*
Saitama, 330-8570, Japan

E-mail: norihiro.iizuka@cern.ch, maeda302@sic.shibaura-it.ac.jp

ABSTRACT: We study the lattice effects on the simple holographic toy model; massive $U(1)$ gauge theory for the bulk action. The mass term is for the $U(1)$ gauge symmetry breaking in the bulk. Without the lattice, the AC conductivity of this model shows similar results to the holographic superconductor with the energy gap. On this model, we introduce the lattice effects, which induce the periodic potential and break the translational invariance of the boundary field theory. Without the lattice, due to the translational invariance and the mass term, there is a delta function peak at zero frequency on the AC conductivity. We study how this delta function peak is influenced by the lattice effects, which we introduce perturbatively. In the probe limit, we evaluate the perturbative corrections to the conductivities at very small frequency limit. We find that the delta function peak remains, even after the lattice effects are introduced, although its weight reduces perturbatively. We also study the lattice wavenumber dependence of this weight. Our result suggests that in the $U(1)$ symmetry breaking phase, the delta function peak is stable against the lattice effects at least perturbatively.

Contents

1 Introduction

Finding the high T_c superconductors on the cuprates system, which are not described by the usual BCS theory, is a remarkable breakthrough in the condensed matter physics occurred almost 26 years ago. Even though there are huge developments after that, both theoretically and experimentally, we are still missing the core mechanism governing the system. One of the common mysterious phenomena in these superconductivity is its Non-Fermi-liquid behavior above the superconducting phase, which occurs near the quantum critical point. The main difficulty to understand the mechanism of these high T_c superconductor is, of course, its strongly coupled dynamics and its lack of the normal quasi-particle pictures. We do not yet fully understand by what mechanism and for what materials, how high T_c superconductor can occur in nature. However, as is recent discovery of iron-based superconductor, experimental progresses on this field are remarkable. These include recent developments of the cold atom experiments. Therefore it can happen that in the near future, we get more crucial experimental data which helps to deepen our understanding of the core mechanism.

On the other hand, one of the most surprising development coming from the string theory is the realization of holographic principle, which states that two totally different theories, string (or gravitational) theories in asymptotically anti-de Sitter space background and strongly coupled large N gauge theories, are equivalent at some limit [1–3]. Recent developments of the holography by applying that to the strongly coupled condensed matter system, is just tremendous.[1] Especially the construction of the holographic superconductor (superfluid) [8–10], where the U(1) symmetry breaking through the hairy black hole in the bulk, intrigues the many interesting developments. See, for examples, [11, 12] for the review of the holographic superconductors.

---

[1]See for examples, [4–7].

In the real-world materials, it happens quite frequently that the materials showing the superconducting phase do not have a translational invariance and Lorentz symmetry, due to the crystal structure of the background atoms. In high T_c superconductor, the effects of the background atomic structure are very important and it is expected that two-dimensional structure plays the significant role. One of the very important effects of the background atomic lattice is that it violates the translational invariance and Lorentz invariance and induces the periodic potential.

If the material possesses a translational invariance and a net charge, it is more or less guaranteed that its electric conductivity shows the delta function peak at zero frequency. This is simply because of the fact that the charged objects are kept accelerated by the outer electric field in a translationally invariant system. We can also understand this from the fact that by the Lorentz boost, the system acquires a nonzero current with zero applied electric field. However, once we break the translational invariance by the lattice, then, there is no guarantee that such a zero frequency delta function peak appears on the conductivity.[2] Therefore it is quite interesting to consider how the delta function peak in many interesting holographic system is influenced by these lattice effects. This is because it is crucial that superconductor possesses such a zero frequency delta function peak even with lattice effects, to have an infinite DC conductivity. In this paper, we take a first step towards the lattice effects on the holographic superconductor; we study the lattice effects on a toy model, which is massive U(1) gauge theory for the bulk action. The mass term of gauge boson is for the U(1) gauge symmetry breaking in the bulk.

Our toy model, although it is a different theory from the holographic superconductor model analyzed by [9, 10], has properties which is similar to the holographic superconductor; Without the lattice, it shows the mass gap, and AC conductivity is quite similar to the results of [9]. It also shows the delta function peak at zero frequency. Therefore, we find it interesting to ask how the zero frequency delta function peak in our model, which is due to the translational invariance and the mass term, is influenced by the lattice effects. Since in our model the gauge boson has mass term, corresponding to the U(1) symmetry breaking of the superconductor (superfluid) phase, this analysis is a first step to study the generic lattice effects on the holographic superconductor phase.

In this paper, we focus on the low frequency limit of the AC conductivity to see if zero frequency delta function peak survives after the lattice effects are introduced. Note that even though zero frequency delta function peak is sensitive to the lattice effects, the lattice effects are expected to be small in the very high frequency limit. This is because, under the very high frequency limit, the degrees of freedom in the system will be excited and obtain the energy which scales as $\propto \omega^2$. However this scale is much bigger than the typical energy scale of the lattice, which scales as $\propto 1/q^2$, where q is the wavenumber of the lattice. Therefore, in the $\omega \to \infty$ limit, the lattice effects are negligible. Therefore interesting phenomena by the lattice effects are in the low frequency and also in the intermediate frequency regime of the AC conductivity.

---

[2]Even if the system has a translational invariance, if we apply magnetic field, this delta function peak disappears. This is because momentum is not conserved in the presence of magnetic field. The same is true in the presence of disorder. See, for example, [13, 14] for the explicit examples of these in the holographic conductivity calculations.

There are several technical points which are worth quoted at this stage. In this paper, we consider the probe limit, namely we neglect the effects of the gravity. It is known that in the normal phase (*i.e.*, non-superconducting phase) without taking into account the gravity, conductivity becomes trivial and there is no delta function peak appearing. The delta function peak appears only if we take into account the gravity effects in the normal phase. On the other hand, in the superconducting phase of [9], the delta function peak appears without taking into account the gravity effects, so is our bulk massive U(1) gauge model. In this paper, without taking into account the gravity, we study how the delta function peak in our model is influenced if we introduce the lattice effects (periodic disturbance to the system) perturbatively.

Before we end this introduction, we comment on several closely related references. Recently there are developments to take into account the lattice effects for the holographic condensed matter system. In the paper by Maeda, Okamura, and Koga [15], the geometry, where the back reaction of lattice effects is taken into account perturbatively, is constructed. In that paper, the lattice effects are introduced through the chemical potential. In [16], Horowitz, Santos, and Tong calculated the conductivity under the presence of the lattice for the *normal* phase, namely, non-superconducting phase. They showed, using a very powerful numerical technique, how the AC conductivity, especially the zero frequency delta function peak, is influenced by the lattice effects. They showed that the delta function peak disappears by the lattice effects, as is expected for the properties of the normal phase. In that paper, the lattice effects are introduced through the neutral scalar field, without relying on the perturbation. Very recently, a paper [17] by Liu, Schalm, Sun, Zaanen, appears where on the geometry without gravitational back reaction, they discussed the lattice effects for the holographic fermion correlators, especially its pole for the Non-fermi-liquids, to see how their dissipation relations are modified.

2 Massive U(1) gauge boson model

2.1 The model

In this paper we consider the following toy model of holographic superconductor for the bulk action.

$$S = \int d^4x \sqrt{-g} \left(-\frac{1}{4}F^2 - V(u,x)A^2 \right),$$ (2.1)

where $V(u,x)$ is external potential, and plays the role of position-dependent mass term for the gauge boson A_μ. u is radial coordinate in the bulk and x is the spatial coordinate in the boundary theory. In more realistic holographic superconductor model, $V(u,x)$ is given by the condensation of the charged scalar field Ψ as [8–10]. There, the massless U(1) gauge boson couples to the charged scalar Ψ, where Ψ takes non-zero VEV, $\Psi^{background}$

$$\Psi = \Psi^{background}(u,x) \neq 0.$$ (2.2)

This gives the potential

$$V(u,x) \sim |\Psi^{background}|^2.$$ (2.3)

corresponding to the spontaneous U(1) symmetry breaking in the bulk, which is dual to the global U(1) symmetry breaking in the boundary theory. However in this paper, we consider $V(u,x)$ as given input for the symmetry breaking. Especially, we consider $V(u,x)$ which satisfies

$$V(u,x) \to 0 \quad \text{(at the boundary),} \tag{2.4}$$

so that at the boundary, the mass term $V(u,x)$ for the gauge boson disappears. We would like to calculate the AC conductivity through the bulk U(1) dynamics A_μ, and discuss the delta function peak with the lattice effects.

One of the main reasons why we consider this toy model is its simplicity. By restricting the degrees of freedom, the calculation for the AC conductivity, especially by choosing appropriate boundary condition, becomes much simpler than the holographic superconductor model in [9, 10]. However, as we will show later, this model, without the lattice, shows the AC conductivity which is quite similar to the one of the holographic superconductor model. It shows the energy gap. Since one of the essential features of the holographic superconductor model is the U(1) symmetry breaking in the bulk, we expect this bottom-up model captures some of the essential features. In this paper, we consider the lattice effects on this model.

The equations of motion for gauge field become

$$\nabla_\nu F^{\mu\nu} = \frac{1}{\sqrt{-g}} \partial_\nu(\sqrt{-g} F^{\mu\nu}) = -2V(u,x)A^\mu, \quad F_{\mu\nu} = \nabla_\mu A_\nu - \nabla_\nu A_\mu. \tag{2.5}$$

We give, by hand, the non-zero arbitrary VEV for the background gauge potential A_μ as

$$A_\mu = A_\mu^{background}(u,x) \neq 0, \tag{2.6}$$

which should be correlated with the nonzero VEV of the charged scalar field (2.2) in holographic superconductor [9, 10]. This nonzero VEV produces a net charge for the boundary theory through the normalizable mode of $A_\mu^{background}$. On this background, in order to calculate the conductivity, we will add small fluctuations given by the ansatz

$$\delta A_\mu dx^\mu = \delta A_t(t,u,x)dt + \delta A_x(t,u,x)dx + \delta A_u(t,u,x)du. \tag{2.7}$$

From the dynamics of these fluctuations δA_μ, we would like to calculate the AC conductivity. However, since the U(1) gauge boson equations of motion are linear equations, all of our analysis are independent on the VEV of the gauge boson (2.6). Therefore our argument for the calculations of the conductivity is independent on the background VEV (2.6).

We take the background metric to be

$$ds^2_{background} = \frac{L^2}{u^2}\left(-h(u)dt^2 + dx^2 + dy^2 + \frac{du^2}{h(u)}\right), \tag{2.8}$$

where h is radial dependent function, given by

$$h(u) = 1 - u^3, \tag{2.9}$$

corresponding to the Schwarzschild AdS black brane.

We study the lattice effects on our model given by the action (2.1). As we quoted already, this model is a different theory from the holographic superconductor one [9], where the degrees of freedom is U(1) gauge boson and the charged scalar field. We give the U(1) symmetry breaking background by hand as (2.2) and (2.6). We have not taken into account the dynamics of the charged scalar field fluctuation in the U(1) symmetry breaking phase, which might not be consistent from the original gauge boson and charged scalar field theory in the bulk. Therefore the reader may regard our model a rather toy model akin to the U(1) symmetry breaking phase of the holographic superconductor. Although our massive U(1) gauge boson model is different model, there are several merit to study this model. First, due to the lack of the dynamical charged scalar, the analysis of solving the equations of motion is simpler in this model. Second, even though we will not take into account the charged scalar field fluctuation for the conductivity calculation, the results of conductivity without the lattice in our model are quite similar to the superconductor model, it shows the mass gap. Technically, this is because charged scalar fluctuation does not directly couple to the gauge boson fluctuation without the lattice. Third, this simple model also shows the zero frequency delta function peak in the probe limit of the holographic superconductor. Therefore even though this model is different, since this model shows very similar properties to the U(1) symmetry breaking phase of the holographic superconductor, we regard this model belongs to the same category to the one in [9]. Therefore even in this model, there are interesting questions we can ask. In this paper, we restrict our attention to this model, and we study the lattice effects on it.

We also point out that in this work, we neglect gravitational back reaction. Once we take into account for the back reaction, the metric will be modified either into Reissner Nordström AdS type of brane or AdS hairy black brane solution. We expect that even if we go beyond the probe limit, the back reaction does not change the picture drastically as is seen explicitly in the case of holographic superconductivity [9, 10]. This is because the most essential feature is not the gravitational back reaction but rather the U(1) symmetry breaking, which we will take into account in this paper. For this reason, we take the background to be Schwarzschild AdS black brane as (2.8), even though there are non-trivial background flux (2.6), to simplify the calculation.

2.2 Generic analysis

We would like to consider the gauge boson fluctuation so that we can obtain AC conductivity. For each of the fluctuation (2.5), the equations of motion becomes

$$h\,\delta A_{t,uu} - (\delta A_{x,tx} - \delta A_{t,xx}) - h\,\delta A_{u,ut} - \frac{2L^2}{u^2}V(u,x)\delta A_t = 0\,, \quad (2.10)$$

$$h\frac{\partial}{\partial u}(h\,\delta A_{x,u}) - (\delta A_{x,tt} - \delta A_{t,xt}) - h\frac{\partial}{\partial u}(h\,\delta A_{u,x}) - \frac{2L^2h}{u^2}V(u,x)\delta A_x = 0\,, \quad (2.11)$$

$$\delta A_{t,tu} - h\,\delta A_{x,xu} - \delta A_{u,tt} + h\,\delta A_{u,xx} - \frac{2L^2h}{u^2}V(u,x)\delta A_u = 0\,. \quad (2.12)$$

Equation of motion for the y component is trivially satisfied by $\delta A_y = 0$.

Clearly, if the potential $V(u,x)$ is independent on position x, then there exists the solution where both $\delta A_t = \delta A_u = 0$ with nontrivial δA_x, which is independent on x.

In such cases, fluctuation equation for δA_x becomes single differential equation for the second order.

Taking the simple time-dependence as $\delta A_i = e^{-i\omega t}a_i$ $(i = t, x, u)$ for the AC conductivity, we obtain

$$h a_{t,uu} + a_{t,xx} + i\omega a_{x,x} + i\omega h a_{u,u} - \frac{2L^2}{u^2}V(u,x)a_t = 0\,, \qquad (2.13)$$

$$h\frac{\partial}{\partial u}(h a_{x,u}) + \omega^2 a_x - i\omega a_{t,x} - h\frac{\partial}{\partial u}(h a_{u,x}) - \frac{2L^2 h}{u^2}V(u,x)a_x = 0\,, \qquad (2.14)$$

$$-i\omega a_{t,u} - h a_{x,xu} + \omega^2 a_u + h a_{u,xx} - \frac{2L^2 h}{u^2}V(u,x)a_u = 0\,. \qquad (2.15)$$

We would like to solve these coupled differential equations by perturbation and obtain the AC conductivity. For that purpose, we add the lattice effects which simply take the following cosine form by the perturbation as

$$V = \frac{1}{L^2}\left(V_0(u) + \epsilon\,\delta V(u)\cos qx\right)\,, \qquad (2.16)$$

where ϵ is a small parameter. $V_0(u)$ corresponds to the homogeneous charged scalar condensation, while $\delta V(u)$ corresponds to the lattice effects. We take the ansatz that the lattice has position x dependence given by the wavenumber q. We will take an explicit example later, but for a moment we keep it generic u-dependent functions $V_0(u)$ and $\delta V(u)$.

We will conduct perturbation expansion for small ϵ as

$$a_x = a_x^{(0)}(\omega,u) + \epsilon a_x^{(1)}(\omega,u)\cos qx + \epsilon^2 a_x^{(2)}(\omega,u,x) + \cdots\,, \qquad (2.17)$$

$$a_t = \epsilon a_t^{(1)}(\omega,u)\sin qx + \epsilon^2 a_t^{(2)}(\omega,u,x) + \cdots\,, \qquad (2.18)$$

$$a_u = \epsilon a_u^{(1)}(\omega,u)\sin qx + \epsilon^2 a_u^{(2)}(\omega,u,x) + \cdots\,. \qquad (2.19)$$

Note that $a_i^{(0)}$ and $a_i^{(1)}$ are independent on x but we keep the implicit x dependence for $a_i^{(2)}$. Then, from (2.13), (2.14), (2.15), we obtain

$$h\frac{d}{du}\left(h\frac{da_x^{(0)}}{du}\right) + \omega^2 a_x^{(0)} - \frac{2hV_0}{u^2}a_x^{(0)} = 0, \qquad (2.20)$$

$$h\frac{d^2}{du^2}a_t^{(1)} - (q^2 a_t^{(1)} + iq\omega a_x^{(1)}) + i\omega h\frac{d}{du}a_u^{(1)} - \frac{2V_0}{u^2}a_t^{(1)} = 0, \qquad (2.21)$$

$$h\frac{d}{du}\left(h\frac{da_x^{(1)}}{du}\right) + \omega^2 a_x^{(1)} - iq\omega a_t^{(1)} - qh\frac{d}{du}(h a_u^{(1)}) - \frac{2hV_0}{u^2}a_x^{(1)} = \frac{2h\delta V}{u^2}a_x^{(0)}, \qquad (2.22)$$

$$-i\omega\frac{d}{du}a_t^{(1)} + qh\frac{d}{du}a_x^{(1)} + \omega^2 a_u^{(1)} - q^2 h\,a_u^{(1)} - \frac{2hV_0}{u^2}a_u^{(1)} = 0\,, \qquad (2.23)$$

$$h\frac{\partial^2}{\partial u^2}a_t^{(2)} + \frac{\partial^2}{\partial x^2}a_t^{(2)} + i\omega\frac{\partial}{\partial x}a_x^{(2)} + i\omega h\frac{\partial}{\partial u}a_u^{(2)} - \frac{2V_0}{u^2}a_t^{(2)} = \frac{2\delta V}{u^2}a_t^{(1)}\sin qx\cos qx\,, \qquad (2.24)$$

$$h\frac{\partial}{\partial u}\left(h\frac{\partial a_x^{(2)}}{\partial u}\right)+\omega^2 a_x^{(2)}-i\omega\frac{\partial}{\partial x}a_t^{(2)}-h\frac{\partial}{\partial u}\left(h\frac{\partial a_u^{(2)}}{\partial x}\right)-\frac{2hV_0}{u^2}a_x^{(2)}=\frac{2h\delta V\cos^2 qx}{u^2}a_x^{(1)}\,,$$

$$(2.25)$$

$$-i\omega\frac{\partial}{\partial u}a_t^{(2)}-h\frac{\partial^2}{\partial u\partial x}a_x^{(2)}+h\frac{\partial^2}{\partial x^2}a_u^{(2)}+\omega^2 a_u^{(2)}-\frac{2hV_0}{u^2}a_u^{(2)}=\frac{2h\delta V}{u^2}a_u^{(1)}\sin qx\cos qx\,.$$

$$(2.26)$$

In order to simplify, we define the average physical quantities over the spatial direction x on the range $2\pi/q$ as

$$\overline{A}(u):=\frac{q}{2\pi}\int_0^{2\pi/q}A(u,x)dx.\qquad(2.27)$$

Then, due to the periodicity of the perturbation along the x direction, (2.25) becomes a simple differential equation as

$$h\frac{d}{du}\left(h\frac{d\overline{a_x^{(2)}}}{du}\right)+\omega^2\overline{a_x^{(2)}}-\frac{2hV_0}{u^2}\overline{a_x^{(2)}}=\frac{h\delta V}{u^2}a_x^{(1)}\,,\qquad(2.28)$$

namely, $\overline{a_x^{(2)}}$ decouples from $\overline{a_t^{(2)}}$, $\overline{a_u^{(2)}}$.

Furthermore in order to impose ingoing boundary condition at the horizon, we re-define the fields as

$$a_i^{(n)}=e^{i\omega u_*}\xi_i^{(n)},\qquad n=0,1,2,\cdots\qquad(2.29)$$

for $i=(t,x,u)$, where

$$u_*\equiv\int^u\frac{du}{h(u)}\,.\qquad(2.30)$$

Then, from (2.20), (2.21), (2.22), (2.28), we obtain

$$h\frac{d^2}{du^2}\xi_x^{(0)}+\left(h'+2i\omega\right)\frac{d\xi_x^{(0)}}{du}-\frac{2V_0}{u^2}\xi_x^{(0)}=0\,,\qquad(2.31)$$

$$h\frac{d^2}{du^2}\xi_t^{(1)}+2i\omega\frac{d\xi_t^{(1)}}{du}+\left[\frac{-i\omega h'}{h}-\frac{\omega^2}{h}-q^2-\frac{2V_0}{u^2}\right]\xi_t^{(1)}$$
$$=iq\omega\xi_x^{(1)}+\omega^2\xi_u^{(1)}-i\omega h\frac{d\xi_u^{(1)}}{du}\,,\qquad(2.32)$$

$$h\frac{d^2}{du^2}\xi_x^{(1)}+\left(h'+2i\omega\right)\frac{d\xi_x^{(1)}}{du}-\frac{2V_0}{u^2}\xi_x^{(1)}$$
$$=\left(iq\omega+qh'\right)\xi_u^{(1)}+qh\frac{d\xi_u^{(1)}}{du}+\frac{iq\omega}{h}\xi_t^{(1)}+\frac{2\delta V}{u^2}\xi_x^{(0)}\,,\quad(2.33)$$

$$\frac{\omega^2}{h}\xi_t^{(1)}-i\omega\frac{d\xi_t^{(1)}}{du}+iq\omega\xi_x^{(1)}+qh\frac{d\xi_x^{(1)}}{du}+\left(\omega^2-q^2h-\frac{2hV_0}{u^2}\right)\xi_u^{(1)}=0\,,\qquad(2.34)$$

$$h\frac{d^2\overline{\xi_x^{(2)}}}{du^2}+\left(h'+2i\omega\right)\frac{d\overline{\xi_x^{(2)}}}{du}-\frac{2V_0}{u^2}\overline{\xi_x^{(2)}}$$
$$=\frac{\delta V}{u^2}\xi_x^{(1)}\,,\qquad(2.35)$$

where $'$ means the u-derivatives. The zeroth order $\xi_i^{(0)}$ gives the conductivity without the lattice effects. By solving (2.31), we can obtain the zeroth order conductivity, $i.e.,$ conductivity without the lattice.

Let us first concentrate on the leading perturbation $\xi_i^{(1)}$. We are interested in the zero frequency delta function peak. For that purpose, it is enough to study the behavior of these equations at low frequency limit. For that purpose, we expand those fields in small ω as

$$\xi_i^{(1)} = \xi_i^{(1),0} + \omega \xi_i^{(1),1} + \omega^2 \xi_i^{(1),2} + \cdots \tag{2.36}$$

for $i = t, x, u$.

Then at the $O(\omega^0)$ order corresponding to the static limit, we have

$$h\frac{d^2}{du^2}\xi_t^{(1),0} + \left(-q^2 - \frac{2V_0}{u^2}\right)\xi_t^{(1),0} = 0, \tag{2.37}$$

$$h\frac{d^2}{du^2}\xi_x^{(1),0} + h'\frac{d\xi_x^{(1),0}}{du} - \frac{2V_0}{u^2}\xi_x^{(1),0} = qh'\xi_u^{(1),0} + qh\frac{d\xi_u^{(1),0}}{du} + \frac{2\delta V}{u^2}\xi_x^{(0),0}, \tag{2.38}$$

$$qh\frac{d\xi_x^{(1),0}}{du} + \left(-q^2 h - \frac{2hV_0}{u^2}\right)\xi_u^{(1),0} = 0. \tag{2.39}$$

Therefore in this static limit $\omega \to 0$, $\xi_t^{(1),0}$ decouples from $\xi_x^{(1),0}$ and $\xi_u^{(1),0}$. Then it is determined by solving the equation (2.37), which gives unique radial coordinate u dependent solution once we give the following two boundary condition; The non-normalizable mode of $\xi_t^{(1),0}$ must vanish at the boundary. $\xi_t^{(1),0}$ must vanish at the horizon, so that Wilson loop

$$e^{\int A_\mu dx^\mu} \sim e^{\int A_\tau d\tau} \tag{2.40}$$

vanishes on the trivial cycle at the horizon, in the Euclid signature. These boundary condition determines that

$$\xi_t^{(1),0} = 0. \tag{2.41}$$

Given this, for the next order $O(\omega^1)$, we have

$$h\frac{d^2}{du^2}\xi_t^{(1),1} + \left(-q^2 - \frac{2V_0}{u^2}\right)\xi_t^{(1),1} = iq\xi_x^{(1),0} - ih\frac{d\xi_u^{(1),0}}{du}, \tag{2.42}$$

$$h\frac{d^2}{du^2}\xi_x^{(1),1} + h'\frac{d\xi_x^{(1),1}}{du} + 2i\frac{d\xi_x^{(1),0}}{du} - \frac{2V_0}{u^2}\xi_x^{(1),1} \tag{2.43}$$

$$= iq\xi_u^{(1),0} + qh'\xi_u^{(1),1} + qh\frac{d\xi_u^{(1),1}}{du} + \frac{2\delta V}{u^2}\xi_x^{(0),1},$$

$$iq\xi_x^{(1),0} + qh\frac{d\xi_x^{(1),1}}{du} + \left(-q^2 h - \frac{2hV_0}{u^2}\right)\xi_u^{(1),1} = 0. \tag{2.44}$$

From (2.39) and (2.44), we can write down $\xi_u^{(1),0}$, $\xi_u^{(1),1}$ in terms of $\xi_x^{(1),0}$, $\xi_x^{(1),1}$ as

$$\xi_u^{(1),0} = \frac{q}{q^2 + \frac{2V_0}{u^2}}\frac{d\xi_x^{(1),0}}{du}, \tag{2.45}$$

$$\xi_u^{(1),1} = \frac{q}{q^2 + \frac{2V_0}{u^2}}\left(\frac{d\xi_x^{(1),1}}{du} + \frac{i}{h}\xi_x^{(1),0}\right). \tag{2.46}$$

These give

$$\xi_u^{(1)} = \frac{q}{q^2 + \frac{2V_0}{u^2}}\left(\frac{d\xi_x^{(1)}}{du} + \frac{i\omega}{h}\xi_x^{(1)}\right) + O(\omega^2).\tag{2.47}$$

From this, it is straightforward to check that at the horizon where $h \to 0$, $\xi_\mu\xi^\mu$ is divergent-free.[3]

By plugging this (2.47) back to the equations (2.32) and (2.33), we obtain differential equations for ξ_t and ξ_x up to order $O(\omega^2)$ accuracy as,

$$h\frac{d^2}{du^2}\xi_t^{(1)} + \left[-q^2 - \frac{2V_0}{u^2}\right]\xi_t^{(1)}$$
$$= iq\omega\xi_x^{(1)} - i\omega h\frac{d}{du}\left(\frac{q}{q^2 + \frac{2V_0}{u^2}}\frac{d\xi_x^{(1)}}{du}\right) + O(\omega^2),\tag{2.53}$$

$$h\frac{d^2}{du^2}\xi_x^{(1)} + \left(h' + 2i\omega\right)\frac{d\xi_x^{(1)}}{du} - \frac{2V_0}{u^2}\xi_x^{(1)}$$
$$= \frac{q\left(iq\omega + qh'\right)}{q^2 + \frac{2V_0}{u^2}}\left(\frac{d\xi_x^{(1)}}{du} + \frac{i\omega}{h}\xi_x^{(1)}\right) + qh\frac{d}{du}\left(\frac{q}{q^2 + \frac{2V_0}{u^2}}\left(\frac{d\xi_x^{(1)}}{du} + \frac{i\omega}{h}\xi_x^{(1)}\right)\right)$$
$$+ \frac{2\delta V}{u^2}\xi_x^{(0)} + O(\omega^2),\tag{2.54}$$

---

[3]To see this, note that by using the regularity of ξ_t at the horizon, (2.42) gives

$$\xi_t^{(1),1} = -\frac{iq}{q^2 + \frac{2V_0}{u^2}}\xi_x^{(1),0}.\tag{2.48}$$

So we have

$$\xi_t^{(1)} = -\omega\frac{iq}{q^2 + \frac{2V_0}{u^2}}\xi_x^{(1),0} + O(\omega^2).\tag{2.49}$$

Therefore, we have, at the horizon where $h \to 0$, neglecting $O(\omega^3)$,

$$\xi_\mu\xi_\nu g^{\mu\nu} = (\xi_t)^2 g^{tt} + (\xi_x)^2 g^{xx} + (\xi_u)^2 g^{uu}$$
$$= \frac{u^2}{L^2}h^{-1}\omega^2\left(\frac{q}{q^2 + \frac{2V_0}{u^2}}\right)^2(\xi_x^{(1),0})^2 + \frac{u^2}{L^2}(\xi_x^{(1),0} + \omega\xi_x^{(1),1} + \omega^2\xi_x^{(1),2})^2$$
$$+ \frac{u^2}{L^2}h\left(\frac{q}{q^2 + \frac{2V_0}{u^2}}\left(\frac{d\xi_x^{(1),0}}{du} + \omega\left(\frac{d\xi_x^{(1),1}}{du} + \frac{i}{h}\xi_x^{(1),0}\right)\right) + \xi_u^{(1),2}\right)^2 + O(\omega^3).\tag{2.50}$$

Here, by using the similar argument, from (2.34), we can see $\xi_u^{(1),2}$ diverges at the horizon as

$$\xi_u^{(1),2} = O(h^{-1}).\tag{2.51}$$

Let's consider the leading divergent terms in above $\xi_\mu\xi_\nu g^{\mu\nu}$. Under the regularity condition for ξ_x, the leading divergent terms which blow up as $O(h^{-1})$ are

$$\xi_\mu\xi_\nu g^{\mu\nu} = \frac{u^2}{L^2}h^{-1}\omega^2\left(\frac{q}{q^2 + \frac{2V_0}{u^2}}\right)^2(\xi_x^{(1),0})^2 + \frac{u^2}{L^2}\omega^2 h\left(\frac{q}{q^2 + \frac{2V_0}{u^2}}\frac{i}{h}\xi_x^{(1),0}\right)^2 + O(h^0).\tag{2.52}$$

So at least up to $O(\omega^2)$, the leading divergent terms, which behave as h^{-1} in $\xi_\mu\xi_\nu g^{\mu\nu}$, cancel.

Note that terms like $\omega\xi_t^{(1)}$ are $O(\omega^2)$. We can solve those equations and resultantly we can determine the conductivity in the low frequency limit. The results allow us to check if zero frequency delta function peak exists or not at this order.

Conductivity is given by

$$\sigma \equiv \frac{A_{x,u}}{F_{xt}} = \frac{a_{x,u}}{a_{t,x} + i\omega a_x}\,, \tag{2.55}$$

which is generically position dependent. Here in numerator, dominant term is a normalizable mode, and in the denominator, dominant term is non-normalizable mode. Expanding A_x and A_t by ϵ, we obtain,

$$\sigma = \sigma^{(0)}(\omega) + \epsilon\cos qx\,\sigma^{(1)}(\omega) + \epsilon^2\sigma^{(2)}(\omega,x) + \cdots \tag{2.56}$$

and

$$\sigma^{(0)}(\omega) = 1 + \frac{\xi_x^{'(0)}(0)}{i\omega\xi_x^{(0)}(0)}\,, \tag{2.57}$$

$$\sigma^{(1)}(\omega) = -\frac{i\xi_x^{'(1)}(0)}{\omega\xi_x^{(0)}(0)} + \frac{i\xi_x^{(1)}(0)\xi_x^{'(0)}(0)}{\omega\xi_x^{(0)}(0)^2} + \frac{iq\xi_t^{(1)}(0)}{\omega\xi_x^{(0)}(0)} + \frac{q\xi_t^{(1)}(0)\xi_x^{'(0)}(0)}{\omega^2\xi_x^{(0)}(0)^2}\,, \tag{2.58}$$

where $'$ is u-derivative. If we look at the spatially averaged part of the conductivity $\overline{\sigma}$ as

$$\begin{aligned}\overline{\sigma(\omega)} &\equiv \frac{q}{2\pi}\int_0^{2\pi/q}\sigma dx \\ &\equiv \overline{\sigma}^{(0)} + \epsilon\overline{\sigma}(\omega)^{(1)} + \epsilon^2\overline{\sigma}(\omega)^{(2)} + \cdots\,,\end{aligned} \tag{2.59}$$

then we obtain,

$$\begin{aligned}\overline{\sigma}^{(1)}(\omega) &= 0, \\ \overline{\sigma}^{(2)}(\omega) &= \frac{\overline{\xi_x^{'(2)}(0)}}{i\omega\xi_x^{(0)}(0)} - \frac{\overline{\xi_x^{(2)}(0)}\xi_x^{'(0)}(0)}{i\omega\xi_x^{(0)}(0)^2} + \frac{q\xi_t^{(1)}(0)\xi_x^{(1)}(0)}{2i\omega\xi^{(0)}(0)^2} + \frac{\xi_x^{(1)}(0)^2\xi_x^{(0)'}(0)}{2i\omega\xi^{(0)}(0)^3} \\ &\quad - \frac{\xi_x^{(1)}(0)\xi_x^{(1)'}(0)}{2i\omega\xi_x^{(0)}(0)^2} - \frac{q^2\xi_t^{(1)}(0)^2}{2\omega^2\xi_x^{(0)}(0)^2} - \frac{q\xi_t^{(1)}(0)\xi_x^{(1)}(0)\xi_t^{(0)'}(0)}{\omega^2\xi_x^{(0)}(0)^3} \\ &\quad + \frac{q\xi_t^{(1)}(0)\xi_x^{(1)'}(0)}{2\omega^2\xi_x^{(0)}(0)^2} - \frac{q^2\xi_t^{(1)}(0)^2\xi_x^{(0)'}(0)}{2i\omega^3\xi_x^{(0)}(0)^3}\,. \end{aligned} \tag{2.60}$$

We would like to evaluate these perturbative corrections to the conductivity by the lattice effects. However, in the real-world experiments, we usually apply a homogeneous electric field and see the conductivity. This means, that we should choose the boundary condition such that inhomogeneous parts of the electric field are set to be zero. This corresponds to choosing non-normalizable modes of the $O(\epsilon)$ terms, $\xi_i^{(1)}(u)$ for $(i = t, x)$, are set to zero

$$\xi_i^{(1)}(0) = 0 \quad , \quad (i = t, x)\,, \tag{2.61}$$

since they have $\cos qx$ dependence. Therefore, above conductivity formula reduces to

$$\sigma^{(1)}(\omega) = -\frac{i\xi_x^{'(1)}(0)}{\omega\xi_x^{(0)}(0)} \quad , \quad \overline{\sigma}^{(2)}(\omega) = \frac{\overline{\xi_x'^{(2)}(0)}}{i\omega\xi_x^{(0)}(0)} - \frac{\overline{\xi_x^{(2)}(0)}\xi_x'^{(0)}(0)}{i\omega\xi_x^{(0)}(0)^2} \,. \qquad (2.62)$$

These are the quantities which we will evaluate.

Without solving the equations of motion explicitly, we can guess how the solution behaves at the zero frequency limit, and therefore, how the zero frequency delta function peak behaves at $\omega \to 0$ limit at this stage.

In the $\omega \to 0$ limit, as we showed in (2.36) and (2.41), we have

$$\xi_t^{(1)} = O(\omega) \quad , \quad \xi_x^{(0)} = O(1) \quad , \quad \xi_x^{(1)} = O(1) \,. \qquad (2.63)$$

Similarly we can also confirm that

$$\xi_x^{(2)} = O(1) \,. \qquad (2.64)$$

Then by plugging these into the perturbative results (2.62), we can obtain that

$$\mathrm{Im}\sigma^{(0)} \sim \frac{1}{\omega} \quad , \quad \mathrm{Im}\sigma^{(1)} \sim \frac{1}{\omega} \quad , \quad \mathrm{Im}\overline{\sigma}^{(2)} \sim \frac{1}{\omega} \,. \qquad (2.65)$$

Therefore we can guess that imaginary of σ has a simple pole structure $\sim \frac{1}{\omega}$, as far as we consider the lattice effect perturbatively. However this argument is very naive, since there is a possibility that the residue of the pole becomes zero and pole disappears. For example, in the normal phase without lattice structure, the above argument breaks down since $\xi_x^{(0)}$ becomes zero therefore the residue of the $\frac{1}{\omega}$ vanish. Therefore in order to confirm above expectation, we will now solve the equations of motion in more explicitly and obtain the solutions. Then, we would like to see if the imaginary of σ has a pole as

$$\mathrm{Im}\,\sigma \sim \frac{1}{\omega} \,. \qquad (2.66)$$

Once this behavior is confirmed, using the Kramers-Kronig relation

$$\mathrm{Im}[\sigma(\omega)] = -\frac{1}{\pi}\mathcal{P}\int_{-\infty}^{\infty} d\omega' \frac{\mathrm{Re}[\sigma(\omega')]}{\omega' - \omega} \,, \qquad (2.67)$$

we can conclude that there is a zero frequency delta function peak. However even if the delta function peak remains, how its residue (weight), $\omega \times \mathrm{Im}\,\sigma$ changes as we vary q is very nontrivial. We will see through the numerical analysis that the weight, which is $\omega \times \mathrm{Im}\,\sigma$, decreases as we increase q.

2.3 Explicit examples for AC conductivities at low frequency limit

In order to work on some explicit examples, let us consider examples where we take

$$V_0 = d_1 u^2(1 + d_2 u^2) \quad , \quad \delta V = u^2 \,. \qquad (2.68)$$

Now we numerically calculate the conductivity $\sigma^{(0)}(\omega)$, $\sigma^{(1)}(\omega)$, $\bar{\sigma}^{(2)}(\omega)$, given by the formula (2.57) and (2.62) for various q in the two typical cases, (i) $d_1 = 5$, $d_2 = 0$ and (ii)
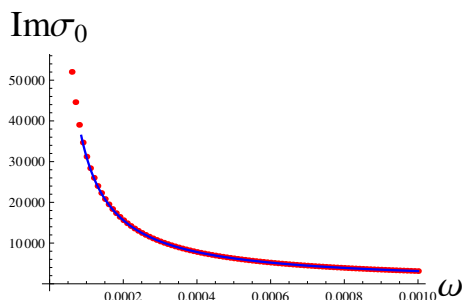
Figure 1. $\text{Im}[\sigma^{(0)}]$ is plotted for various ω (red) in the case (i). The best fitting curve (blue) is $\text{Im}[\sigma^{(0)}(\omega)] \simeq -9.4 \times 10^{-4} + 3.1/\omega$.
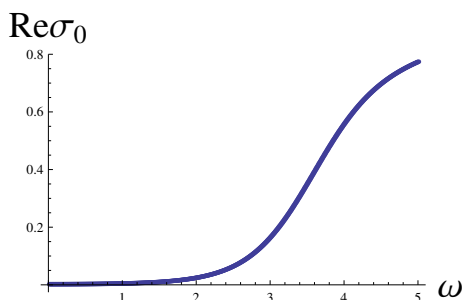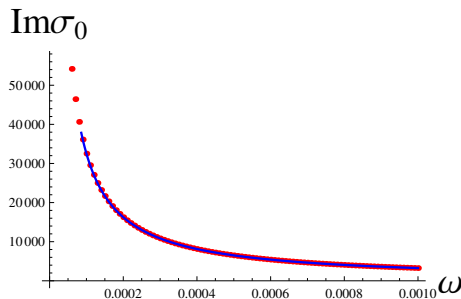

Figure 2. $\text{Re}[\sigma^{(0)}]$ is plotted for various ω in the case (i). There is a delta function peak at $\omega = 0$.

$d_1 = 5$, $d_2 = 2$, respectively. We have chosen the power for V_0 as u^2 and u^4. These choices are due to the fact that the asymptotic behaviors of the background charged scalar, which condensates, behaves as $\Psi^{background} \sim u$ or $\Psi^{background} \sim u^2$, see eq. (8) of [9].

By imposing regularity condition at the horizon,

$$\xi_x^{(0)}(1) = \text{regular}, \tag{2.69}$$

we obtain the conductivity $\sigma^{(0)}(\omega)$ by numerically solving (2.31). Figure 1–4 show $\sigma^{(0)}(\omega)$. As is seen from the figures for the $\text{Re}[\sigma^{(0)}(\omega)]$, for the both cases, the gap appears. The energy gap in figure 4 is larger than the one in figure 2 because the "condensation" $V_0(u) \sim |\Psi^{background}|^2$ in the case (ii) is larger than the one in the case (i). As we mentioned in the introduction, these results for conductivities are quite similar to the conductivity calculations for the holographic superconductor [9]. Especially there are energy gaps and delta function peak at $\text{Re}[\sigma^{(0)}(\omega)] = 0$, which is seen from the imaginary parts of σ_0 behave as $\frac{1}{\omega}$. For in figure 2 and 4, both $\text{Re}[\sigma^{(0)}(\omega)]$ approaches small but nonzero value at $\omega \to 0$, corresponding to the existence of the mass gap.

By Kramers-Kronig relation (2.67), the real part of the conductivity contains a delta function peak such as $\text{Re}[\sigma^{(0)}(\omega)] \simeq \pi C^{(0)} \delta(\omega)$ if the imaginary part of the conductivity contains a pole such as $\text{Im}[\sigma^{(0)}(\omega)] \simeq C^{(0)}/\omega$. Figure 1 and 3 show that the pole exists at $\omega = 0$ for both cases (i) and (ii). The best fitting curves determine the coefficients $C^{(0)}$ as $C^{(0)} = 3.1$ (the case (i)) and $C^{(0)} = 3.25$ (the case (ii)).

Figure 3. $\text{Im}[\sigma^{(0)}]$ is plotted for various ω (red) in the case (ii). The best fitting curve (blue) is $\text{Im}[\sigma^{(0)}(\omega)] \simeq -8.4 \times 10^{-5} + 3.25/\omega$.
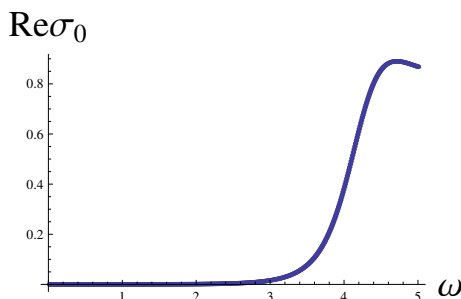

Figure 4. $\text{Re}[\sigma^{(0)}]$ is plotted for various ω in the case (ii). There is a delta function peak at $\omega = 0$.

The first order conductivity $\sigma^{(1)}(\omega)$ is obtained by numerically solving the following equations from (2.53) and (2.54);

$$h\frac{d^2}{du^2}\xi_t^{(1)} + \left[-q^2 - 2d_1(1+d_2u^2)\right]\xi_t^{(1)} \tag{2.70}$$

$$= iq\omega\xi_x^{(1)} - \frac{i\omega h q}{q^2 + 2d_1(1+d_2u^2)}\frac{d^2\xi_x^{(1)}}{du^2} + \frac{4i\omega h q d_1 d_2 u}{(q^2 + 2d_1(1+d_2u^2))^2}\frac{d\xi_x^{(1)}}{du} + O(\omega^2),$$

$$h\frac{d^2}{du^2}\xi_x^{(1)} + \left(h' + 2i\omega\right)\frac{d\xi_x^{(1)}}{du} - 2d_1(1+d_2u^2)\xi_x^{(1)}$$

$$= \left(\frac{q\left(iq\omega + qh'\right)}{q^2 + 2d_1(1+d_2u^2)} - \frac{4d_1 d_2 h q^2 u}{(q^2 + 2d_1(1+d_2u^2))^2}\right)\left(\frac{d\xi_x^{(1)}}{du} + \frac{i\omega}{h}\xi_x^{(1)}\right)$$

$$+ \frac{q^2 h}{q^2 + 2d_1(1+d_2u^2)}\left(\frac{d^2\xi_x^{(1)}}{du^2} + \frac{i\omega}{h}\frac{d\xi_x^{(1)}}{du}\right) - \frac{i\omega q^2 h'}{h\left(q^2 + 2d_1(1+d_2u^2)\right)}\xi_x^{(1)}$$

$$+ 2\xi_x^{(0)} + O(\omega^2), \tag{2.71}$$

To obtain the solution, we need to impose boundary conditions both at the horizon and the infinity. As we mentioned, in real-world experiments, we usually apply a homogeneous electric field and measure the conductivity. Therefore we shall impose a constant electric field condition at infinity. Since $O(\epsilon)$ part of the flux has $\cos qx$ dependence, we require
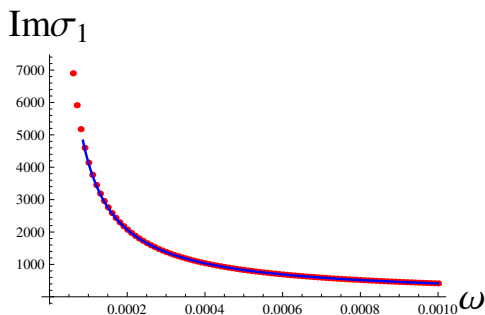
Figure 5. (Color online) $\mathrm{Im}[\sigma(\omega)^{(1)}]$ in the case (i) for $q = 2$. The best fitting curve is $\sigma^{(1)} \simeq 9.2 \times 10^{-5} + 0.41/\omega$.
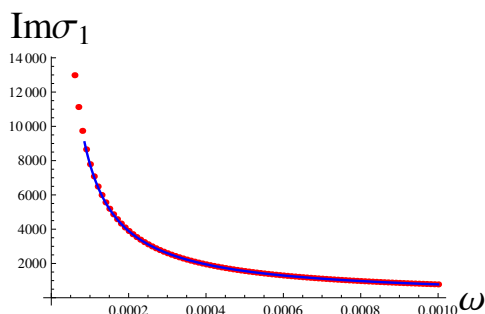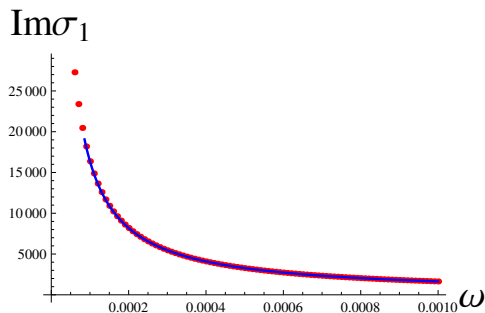

Figure 6. (Color online) $\mathrm{Im}[\sigma(\omega)^{(1)}]$ in the case (i) for $q = 5$. The best fitting curve is $\sigma^{(1)} \simeq 0.0024 + 0.78/\omega$.

that

$$E_x^{(1)}(0) = \left(i\omega a_x^{(1)}(0) + q a_t^{(1)}(0) \right) \cos qx = 0 \,, \tag{2.72}$$

for arbitrary x. We have chosen $\xi_x^{(1)}(0) = \xi_t^{(1)}(0) = 0$ as (2.61), therefore (2.72) is satisfied. We also require that the regularity condition for $\xi_x^{(1)}$ and $\xi_t^{(1)}$ at the horizon, which yield the ingoing condition for $a_x^{(1)}$ and $a_t^{(1)}$.

Figure 5–10 show $\mathrm{Im}[\sigma^{(1)}(\omega)]$ for various wavenumbers $q = 2, 5, 10$ for each case. Let us define the coefficient $\tilde{C}(q)$ as $\mathrm{Im}[\sigma^{(1)}(\omega)] = \tilde{C}(q)/\omega + O(1)$ near $\omega = 0$. Then, the coefficient $\tilde{C}(q)$ can be read from the best fitting curves in figure 5–10 as $\tilde{C}(2) = 0.41, \tilde{C}(5) = 0.78$, and $\tilde{C}(10) = 1.6$ for the case (i), while $\tilde{C}(2) = 0.38, \tilde{C}(5) = 0.73,$ and $\tilde{C}(10) = 1.58$ for the case (ii). This implies that the coefficient $\tilde{C}(q)$ increases as q increases.

Finally, we show q-dependence of $\overline{\sigma}(\omega)^{(2)}$ in figures 11–16. $\overline{\sigma}(\omega)^{(2)}$ is numerically obtained by solving eq. (2.35) under the regularity condition for $\bar{\xi}_x^{(2)}$ at the horizon and the constant electric field condition. Let us expand the imaginary part of the spatially averaged conductivity $\overline{\sigma}$ as

$$\mathrm{Im}[\overline{\sigma}] = \frac{C(q)}{\omega} = \frac{C^{(0)} + \epsilon C^{(1)}(q) + \epsilon^2 C^{(2)}(q) + \cdots}{\omega} + O(1) \tag{2.73}$$

– 14 –

Figure 7. (Color online) $\mathrm{Im}[\sigma(\omega)^{(1)}]$ in the case (i) for $q = 10$. The best fitting curve is $\sigma^{(1)} \simeq 0.72 + 1.6/\omega$.
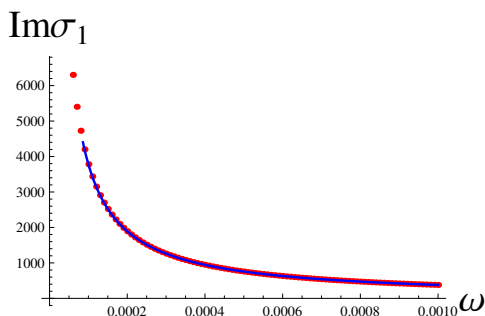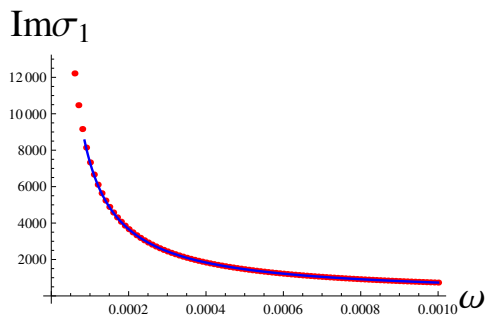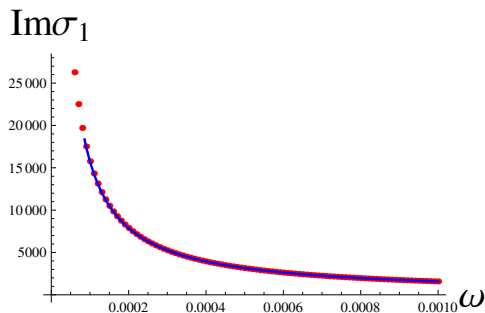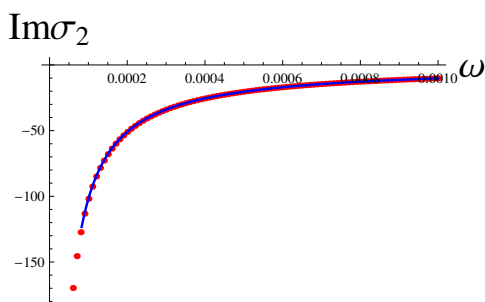

Figure 8. (Color online) $\mathrm{Im}[\sigma(\omega)^{(1)}]$ in the case (ii) for $q = 2$. The best fitting curve is $\sigma^{(1)} \simeq 2.7 \times 10^{-4} + 0.38/\omega$.

Figure 9. (Color online) $\mathrm{Im}[\sigma(\omega)^{(1)}]$ in the case (ii) for $q = 5$. The best fitting curve is $\sigma^{(1)} \simeq 0.0024 + 0.73/\omega$.

near the origin, $\omega = 0$. Then, by definition, we immediately obtain $C^{(1)}(q) = 0$. Therefore, the coefficient $C(q)$ is given by

$$C(q) = C^{(0)} + \epsilon^2 C^{(2)}(q). \tag{2.74}$$

The coefficient $C^{(2)}(q)$ can be read from the best fitting curves as in figure 11–16 as $C^{(2)}(2) = -0.010$, $C^{(2)}(5) = -0.014$, and $C^{(2)}(10) = -0.020$ for the case (i), while $C^{(2)}(2) = -0.0067$, $C^{(2)}(5) = -0.010$, and $C^{(2)}(10) = -0.015$ for the case (ii). Therefore,

– 15 –

Figure 10. (Color online) $\mathrm{Im}[\sigma(\omega)^{(1)}]$ in the case (ii) for $q = 10$. The best fitting curve is $\sigma^{(1)} \simeq 0.49 + 1.58/\omega$.

Figure 11. (color online) $\mathrm{Im}[\sigma(\omega)^{(2)}]$ in the case (i) for $q = 2$. The best fitting curve is $\sigma^{(2)} \simeq -1.3 \times 10^{-6} - 0.010/\omega$.
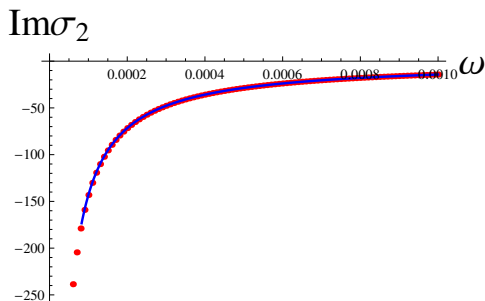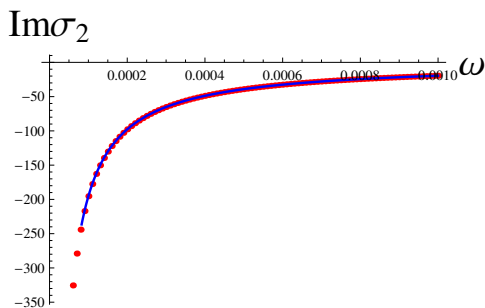

Figure 12. (Color online) $\mathrm{Im}[\sigma(\omega)^{(2)}]$ in the case (i) for $q = 5$. The best fitting curve is $\sigma^{(2)} \simeq -2.5 \times 10^{-6} - 0.014/\omega$.

the lattice effects reduce the coefficient $C(q)$ for any wavenumber q. Furthermore, we find that as q increases, the coefficient $C^{(2)}(q)$, and therefore $C(q)$, decreases.

By Kramers-Kronig relation, the real part of the conductivity contains a delta function peak if the imaginary part of the conductivity contains a pole. All these results suggest that, the magnitudes of the zero frequency delta function peak decrease by the lattice effects. This implies that in the holographic superconductor, the "superfluid component" of the conductivity decreases by the lattice effects.

Figure 13. (Color online) $\text{Im}[\sigma(\omega)^{(2)}]$ in the case (i) for $q = 10$. The best fitting curve is $\sigma^{(2)} \simeq -3.9 \times 10^{-6} - 0.020/\omega$.
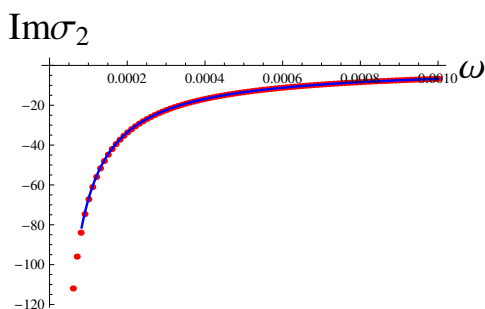

Figure 14. (Color online) $\text{Im}[\sigma(\omega)^{(2)}]$ in the case (ii) for $q = 2$. The best fitting curve is $\sigma^{(2)} \simeq -5.6 \times 10^{-7} - 0.0067/\omega$.
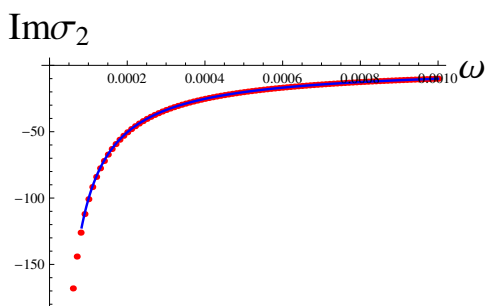

Figure 15. (color online) $\text{Im}[\sigma(\omega)^{(2)}]$ in the case (ii) for $q = 5$. The best fitting curve is $\sigma^{(2)} \simeq 3.5 \times 10^{-7} - 0.010/\omega$.

3 Conclusion and discussion

We studied the lattice effects on the toy model of holographic superconductor (superfluidity), massive U(1) gauge boson model. Especially we studied how the zero frequency delta function peak on the real part of the conductivity is influenced by the lattice effects. Our analysis suggests that even though its weight reduces, the delta-function peak still remains even after the lattice effects are taken into account. This implies that the superfluid component remains with the lattice. We have seen also that, as the wavenumber of the lattice increases, the weight of the delta function peak decreases.
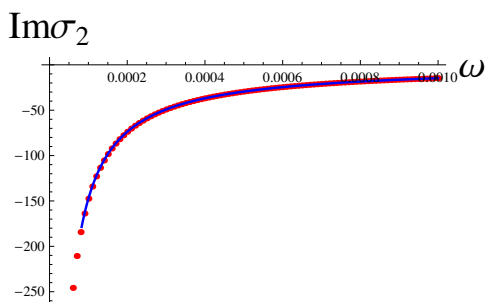
Figure 16. (Color online) $\text{Im}[\sigma(\omega)^{(2)}]$ in the case (ii) for $q = 10$. The best fitting curve is $\sigma^{(2)} \simeq 0.00015 - 0.015/\omega$.

However in order to get conclusive results, clearly we need to study things in more great detail. In our toy holographic superconductivity (superfluidity) model, we have neglected two important ingredients, the dynamics of the charged scalar field and also the gravity. For the charged scalar field, instead of treating it as a dynamical field, we have given its VEV by hand as an input. This nonzero VEV corresponds to the U(1) symmetry breaking and yields the mass term for the gauge boson. Even though we vary this VEV and its radial profile through the several parameters of our system, we have seen that the zero frequency delta function peak remains. Therefore, we expect that the results will not be modified much even after we have taken into account the charged scalar dynamics. However of course, it is better to confirm this point in more explicitly by taking into account the dynamics of the charged scalar field.

We have also neglected the effects of the gravity. There are two important effects associated with the gravity dynamics; The first one is the back reaction of the lattice effects to the geometry, since we have used the background geometry which does not possess the lattice effects. This correction can be calculated perturbatively, as is studied, for example, in [15]. This induces the perturbative corrections to the background geometry, and how the perturbative correction appears on the geometry depends on how we introduce it. Suppose the lattice effects are $O(\epsilon)$, then, depending on the lattice effects which appear to the energy-momentum tensor at either $O(\epsilon)$ or $O(\epsilon^2)$, the order of back reaction to the geometry is different. If we introduce the perturbative lattice effects on the chemical potential as [15] to the background with nonzero chemical potential background, then the back reaction of the lattice effects appear as $O(G_N \epsilon)$, then it cannot be neglected unless we take the probe limit. On the other hand, if we introduce the perturbative lattice effects by introducing neutral scalar field as [16], then its back reaction appears as $O(G_N \epsilon^2)$ therefore it can be neglected at the leading order in ϵ without taking the probe limit.

There is also gravity effects on the conductivity calculations. As we quote in the introduction, the delta function peak does not appear in the normal phase, where U(1) symmetry is preserved. This can be seen for example, by the fact that without gravity effect, on the normal phase, the equations of motion for the gauge boson A_μ admits only trivial constant solution.[4] Once we take into account the gravity, we can see the delta

---

[4]In fact if we re-write the equations of motion for the gauge boson A_μ as Schrodinger equation and
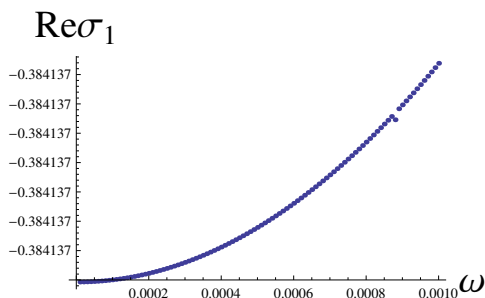
Figure 17. (Color online) $\mathrm{Re}[\overline{\sigma(\omega)^{(1)}}]$ in the case of $d_1 = 5$, $d_2 = 0$, $q = 2$.

function peak, originated from the translational invariance of the system. In [16], by taking into account the gravity effect, it is shown that the zero frequency delta function peak becomes flatten once we take into account the lattice effects. It is interesting to see how the results in this paper are influenced if we take into account the gravity effect.

Finally even if we take into account all of above effects, it is not clear if the perturbative analysis, as we have done in this paper, is enough to give us conclusive results. It is possible that there are non-perturbative corrections to the conductivity by the lattice effects, which significantly influence the delta function peak. In such cases, we may have to rely fully on the numerical analysis. We left these open questions for the future projects.

Acknowledgments

A A real part of the conductivity

In this appendix, we summarize the numerical data for the real part of the conductivity. In figures 2 and 4, we show the $\mathrm{Re}[\sigma(\omega)^{(0)}]$ in the case of $d_1 = 5$, $d_2 = 0$ and $d_1 = 5$, $d_2 = 2$, respectively. It is clear that there is an energy gap approximately in the region $0 \leq \omega \leq 3$ for both cases.

In figures 17–22, $\mathrm{Re}[\sigma(\omega)^{(i)}]$ $(i = 1, 2)$ are plotted in the case of $d_1 = 5$, $d_2 = 0$ and $d_1 = 5$, $d_2 = 2$, respectively for each $q = 2, 5$. In any case, the real part approaches a constant in the limit $\omega \to 0$.

Note that even though $\mathrm{Re}[\sigma(\omega)^{(i)}] < 0$ $(i = 1, 2)$, since we have small but nonzero $\mathrm{Re}[\sigma(\omega)^{(0)}] > 0$, as long as we consider the perturbative analysis, the real part of the conductivities are always positive.

---

treating the calculation for the conductivity as scattering problem [18], the potential vanishes if we neglect the gravity effect on the normal phase. Therefore the conductivity is always unity, and we cannot see any delta function peak.
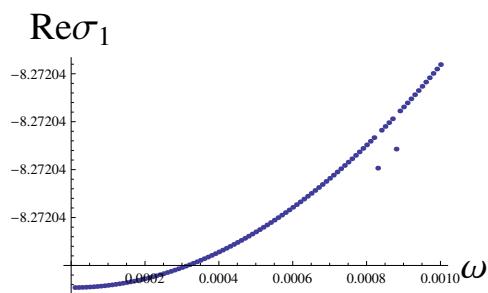
Figure 18. (Color online) $\mathrm{Re}[\overline{\sigma(\omega)^{(1)}}]$ in the case of $d_1 = 5$, $d_2 = 0$, $q = 5$.
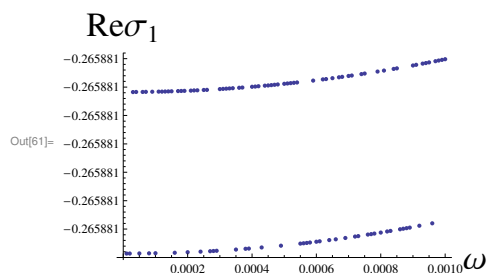

Figure 19. (Color online) $\mathrm{Re}[\overline{\sigma(\omega)^{(1)}}]$ in the case of $d_1 = 5$, $d_2 = 2$, $q = 2$.
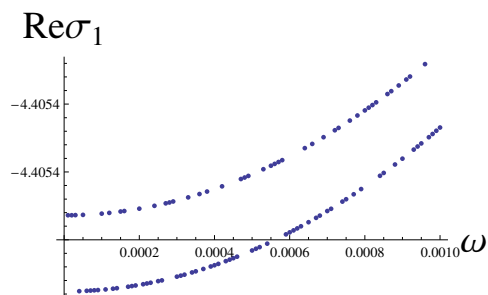

Figure 20. (Color online) $\mathrm{Re}[\overline{\sigma(\omega)^{(1)}}]$ in the case of $d_1 = 5$, $d_2 = 2$, $q = 5$.
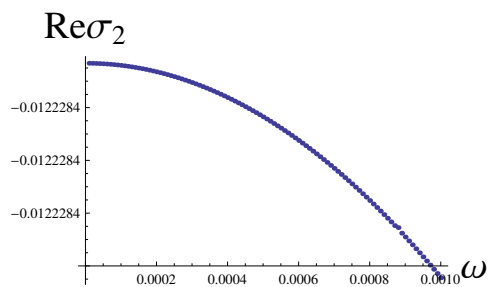

Figure 21. (Color online) $\mathrm{Re}[\overline{\sigma(\omega)^{(2)}}]$ in the case of $d_1 = 5$, $d_2 = 0$, $q = 2$.
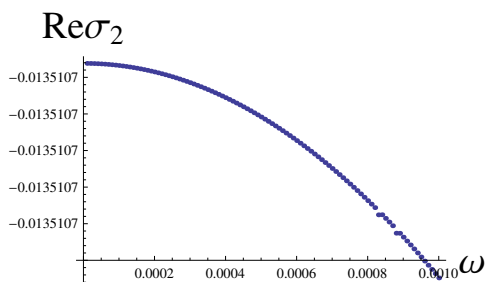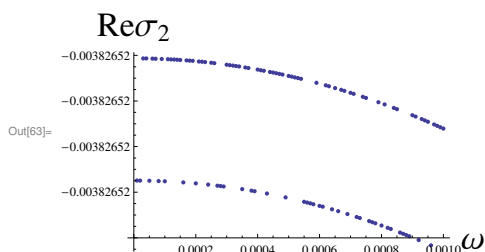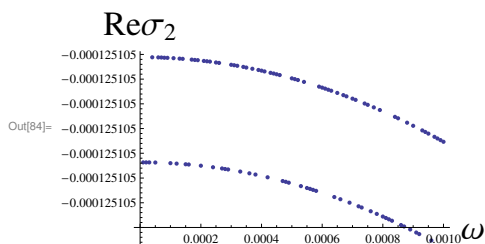
Reσ_2

−0.0135107
−0.0135107
−0.0135107
−0.0135107
−0.0135107

0.0002　0.0004　0.0006　0.0008　0.0010　ω

Figure 22. (Color online) $\mathrm{Re}[\overline{\sigma(\omega)^{(2)}}]$ in the case of $d_1 = 5$, $d_2 = 0$, $q = 5$.

Reσ_2

−0.00382652
−0.00382652
Out[63]=　−0.00382652
−0.00382652

0.0002　0.0004　0.0006　0.0008　0.0010　ω

Figure 23. (Color online) $\mathrm{Re}[\overline{\sigma(\omega)^{(2)}}]$ in the case of $d_1 = 5$, $d_2 = 2$, $q = 2$.

Reσ_2

−0.000125105
−0.000125105
−0.000125105
Out[84]=　−0.000125105
−0.000125105
−0.000125105

0.0002　0.0004　0.0006　0.0008　0.0010　ω

Figure 24. (Color online) $\mathrm{Re}[\overline{\sigma(\omega)^{(2)}}]$ in the case of $d_1 = 5$, $d_2 = 2$, $q = 5$.

References

[1] J.M. Maldacena, *The large-N limit of superconformal field theories and supergravity*, *Adv. Theor. Math. Phys.* **2** (1998) 231 [*Int. J. Theor. Phys.* **38** (1999) 1113] [`hep-th/9711200`] [INSPIRE].

[2] E. Witten, *Anti-de Sitter space and holography*, *Adv. Theor. Math. Phys.* **2** (1998) 253 [`hep-th/9802150`] [INSPIRE].

[3] S. Gubser, I.R. Klebanov and A.M. Polyakov, *Gauge theory correlators from noncritical string theory*, *Phys. Lett.* **B 428** (1998) 105 [`hep-th/9802109`] [INSPIRE].

[4] S.A. Hartnoll, *Lectures on holographic methods for condensed matter physics*, *Class. Quant. Grav.* **26** (2009) 224002 [`arXiv:0903.3246`] [ɪɴSPIRE].

[5] J. McGreevy, *Holographic duality with a view toward many-body physics*, *Adv. High Energy Phys.* **2010** (2010) 723105 [`arXiv:0909.0518`] [ɪɴSPIRE].

[6] S. Sachdev, *Condensed matter and AdS/CFT*, `arXiv:1002.2947` [ɪɴSPIRE].

[7] S.A. Hartnoll, *Horizons, holography and condensed matter*, `arXiv:1106.4324` [ɪɴSPIRE].

[8] S.S. Gubser, *Breaking an abelian gauge symmetry near a black hole horizon*, *Phys. Rev.* **D 78** (2008) 065034 [`arXiv:0801.2977`] [ɪɴSPIRE].

[9] S.A. Hartnoll, C.P. Herzog and G.T. Horowitz, *Building a holographic superconductor*, *Phys. Rev. Lett.* **101** (2008) 031601 [`arXiv:0803.3295`] [ɪɴSPIRE].

[10] S.A. Hartnoll, C.P. Herzog and G.T. Horowitz, *Holographic superconductors*, *JHEP* **12** (2008) 015 [`arXiv:0810.1563`] [ɪɴSPIRE].

[11] C.P. Herzog, *Lectures on holographic superfluidity and superconductivity*, *J. Phys.* **A 42** (2009) 343001 [`arXiv:0904.1975`] [ɪɴSPIRE].

[12] G.T. Horowitz, *Introduction to holographic superconductors*, `arXiv:1002.1722` [ɪɴSPIRE].

[13] K. Goldstein et al., *Holography of dyonic dilaton black branes*, *JHEP* **10** (2010) 027 [`arXiv:1007.2490`] [ɪɴSPIRE].

[14] K. Maeda and T. Okamura, *Vortex flow for a holographic superconductor*, *Phys. Rev.* **D 83** (2011) 066004 [`arXiv:1012.0202`] [ɪɴSPIRE].

[15] K. Maeda, T. Okamura and J.-i. Koga, *Inhomogeneous charged black hole solutions in asymptotically Anti-de Sitter spacetime*, *Phys. Rev.* **D 85** (2012) 066003 [`arXiv:1107.3677`] [ɪɴSPIRE].

[16] G.T. Horowitz, J.E. Santos and D. Tong, *Optical conductivity with holographic lattices*, *JHEP* **07** (2012) 168 [`arXiv:1204.0519`] [ɪɴSPIRE].

[17] Y. Liu, K. Schalm, Y.-W. Sun and J. Zaanen, *Lattice potentials and fermions in holographic non Fermi-liquids: hybridizing local quantum criticality*, *JHEP* **10** (2012) 036 [`arXiv:1205.5227`] [ɪɴSPIRE].

[18] G.T. Horowitz and M.M. Roberts, *Zero temperature limit of holographic superconductors*, *JHEP* **11** (2009) 015 [`arXiv:0908.3677`] [ɪɴSPIRE].